IEEE Access
Multidisciplinary ⋮ Rapid Review ⋮ Open Access Journal

Received November 23, 2021, accepted January 7, 2022, date of publication January 14, 2022, date of current version January 26, 2022.

Digital Object Identifier 10.1109/ACCESS.2022.3143583

Performance of Priority-Based Traffic Coexistence Strategies in 5G mmWave Industrial Deployments

DARIA IVANOVA[1], EKATERINA MARKOVA[1], DMITRI MOLTCHANOV[2], RUSTAM PIRMAGOMEDOV[2], YEVGENI KOUCHERYAVY[3], AND KONSTANTIN SAMOUYLOV[1,4]

[1]Department of Applied Probability and Informatics, Peoples' Friendship University of Russia (RUDN University), 117198 Moscow, Russia
[2]Tampere University, 33720 Tampere, Finland
[3]Kharkevich Institute for Information Transmission Problems, Russian Academy of Sciences, 127051 Moscow, Russia
[4]Federal Research Center "Computer Science and Control," Russian Academy of Sciences, 119333 Moscow, Russia

Corresponding author: Dmitri Moltchanov (dmitri.moltchanov@tuni.fi)

This work was supported in part by the Russian Science Foundation (https://rscf.ru/en/project/21-19-00846/) under Grant 21-19-00846, in part by the Russian Science Foundation through the Sections I and II (https://rscf.ru/en/project/21-79-10139/) under Grant 21-79-10139, and in part by the Peoples' Friendship University of Russia (RUDN) University Strategic Academic Leadership Program (recipients Ekaterina Markova and Daria Ivanova, Section IV and V).

ABSTRACT Recently standardized New Radio (NR) technology supports both ultra-reliable low-latency (URLLC) service and conventional enhanced mobile broadband (eMBB) service. Owing to extreme latency and reliability requirements an explicit prioritization needs to be provided to URLLC service when these traffic types are mixed up at the air interface. In this work, we consider simultaneous support of these two services in an industrial environment, where production line equipment utilizes URLLC service for reorganization and synchronous operation while eMBB service is used for remote monitoring. By utilizing the tools of stochastic geometry and queuing theory, we formalize the model with pre-emptive priority service at NR base station (BS) with and without direct device-to-device (D2D) communications. Our numerical results indicate that the priority-based implementation of URLLC and eMBB coexistence allows us to isolate the former traffic efficiently and requires no external control. D2D-aware strategy, where the BS explicitly reserves some resources for direct communications, drastically outperforms those, where no explicit reservation is utilized, as well as the baseline strategy where all the traffic goes through the BS. This strategy can achieve 10^{-5} of URLLC drop probability when the baseline strategy produces just 5×10^{-3}, leading to three orders of magnitude reduction in drop probability and without significant impact produced on eMBB session drop probability. The developed model can be utilized to estimate the NR BS density required to support prescribed performance guarantees for all the considered strategies.

INDEX TERMS 5G, industrial NR, new radio, priority service, URLLC.

I. INTRODUCTION

Fifth-generation (5G) mobile systems have been developed with an large scope of applications in mind [1]. One of the most prominent 5G use-cases characterized by complex deployment conditions and extreme service requirements is industrial automation scenarios [2], [3].

In industrial automation scenarios, 5G NR is expected to enable a large range of services, such as the joint operation of mobile robots, wireless time synchronization, positioning, augmented reality services for personnel, and telepresence-based maintenance operation [3], [4]. The systems that control the moving elements of manufacturing equipment commonly generate low-rate traffic but require ultra-reliable low-latency service (URLLC) while video-guided machinery or mobile robots require enhanced mobile broadband (eMBB) service [1]. Thus, NR BSs need to support a mixture of eMBB and URLLC services at the same time. Mechanisms for supporting these services in isolation at mmWave NR BSs are currently the focus of ongoing

The associate editor coordinating the review of this manuscript and approving it for publication was Ding Xu.

studies, e.g., [5]–[7] for eMBB and [8]–[10] for URLLC. Specifically, in context of URLLC service, packet duplication allowing to provide high level of reliability for URLLC services is considered in [9]. However, the authors show that it is beneficial only in certain scenarios with unfavorable channel conditions. With respect to eMBB traffic, the authors in [6] improve session-level reliability by utilizing resource reservation technique. Alternative approach based on multiconnectivity functionality is considered in [8]. However, only a few studies assess the joint support of these traffic types at 5G mmWave BSs.

A. RELATED WORK

To enable coexistence between URLLC and eMBB traffic a number of approaches have been considered. The authors of the paper [11] proposed to solve the problem of multiplexing eMBB and URLLC traffic in the uplink channel by a novel flexible scheme that is based on non-orthogonal multiple access (NOMA). According to the scheme, they developed a scheduling and power allocation algorithm for eMBB services that considers the constraints imposed by URLLC transmissions. The authors evaluated the performance of the proposed scheme using computer simulations and showed that it allows to increase throughput for the eMBB services while satisfying strict quality of service (QoS) requirements for the URLLC ones. NOMA inspired techniques also considered in [12]–[15], but in these cases the authors propose to use network slicing to meet the requirements of each service, where each service gets resources to provide performance guarantees and isolation from the other services. Specifically, in [12], the authors proposed the use of NOMA to improve the number of URLLC services that are connected in the uplink to the same base station (BS), for both orthogonal and non-orthogonal network slicing with eMBB services. In [13], the authors considered the potential advantages of allowing for non-orthogonal sharing of radio access network (RAN) resources in uplink direction from a set of eMBB, mMTC, and URLLC services. The inherent advantage of NOMA approach is that the latency critical data can be scheduled immediately without waiting for the beginning of the next scheduling interval. However, it requires complex design of the forward error correction mechanism and the choice of the affected resource blocks.

As NOMA is not supported in by the current evolution of 5G NR standards, the resource reservation technique for simultaneous support of URLLC and eMBB traffic over the NR air interface has been proposed [13], [16]. Particularly, the authors in [17] proposed to reserve random access resources for URLLC traffic during the initial random access transmission. For this purpose, an improved random access mechanism for different reservation policies has been developed. By utilizing the computer simulations, the authors demonstrated that the proposed technique can meet the 10 ms delay constraint with 95% confidence. However, as the traffic arrival intensities may not be known in advance, this approach may result in inefficient use of resources. To improve efficiency of resource reservation mechanism, one needs to design lightweight and accurate traffic prediction algorithm that would dynamically change the amount of resources allocated to the traffic types at the scheduling time horizon, which is 1 ms for NR [18]. In [19] a proactive resource reservation scheme has been proposed. To reduce the impact on eMBB traffic performance, the authors applied the vehicle trajectory prediction algorithm and demonstrated that limiting reservation to fewer cells allows reaching the URLLC QoS with a reduced impact on the network capacity. In [20], key requirements of URLLC are considered. To meet these requirements, the authors studied in detail the scheduling schemes, in particular, reservation-based scheduling [21], namely, semi-static and dynamic reservations. Their results demonstrated that dynamic reservation outperforms semi-static reservation in terms of latency due to the fast resource allocation adaptation.

Alternatively, to dynamically distribute air interface resources between types, one may also utilize priority-based scheduling. In this case, if the arrival intensity of either URLLC or eMBB traffic increases resulting in congestion, one or more session of the latter traffic type can be dropped. In our previous studies [22], [23], we developed a model for performance assessment of this strategy and demonstrated that explicit prioritization may indeed lead to almost perfect resource utilization while delivering the required performance guarantees to URLLC traffic. This approach has also been studies in [24], where system- and link-level simulations demonstrated the performance benefits of this mechanism. The methods considered by the authors are shown to efficiently reduce the latency, may not adapt dynamically for time-varying traffic dynamics. In the paper [25], the authors proposed to formalize resource scheduling over a time slot. For this purpose, they suggested a puncturing technique for URLLC traffic over the scheduled resources, and considered the sequential scheduling scenario for the preempted eMBB users in the next time-slot. The carried our simulation study showed the efficacy of the dynamic scheduling method. Further, in [26], the authors proposed a null-space-based spatial preemptive scheduler for URLLC and eMBB traffic coexistence [27]. The considered framework utilizes the system's spatial degrees of freedom to instantly offer an interference-free subspace for URLLC traffic. This allows preserving a sufficient URLLC decoding ability with minimal impact on the eMBB performance. The authors conducted analysis and extensive system-level simulations showing that the scheduler offers robust URLLC latency performance with a significantly improved capacity.

Resource scheduling for URLLC traffic support has been addressed in [28]. The main purpose of the work was to formalize and solve the optimization problem, aimed at maximizing the eMBB data transfer rate, by taking into account the URLLC reliability requirements. The authors considered two timescales of interest, time slot, where resource allocation for eMBB is performed, and subslot, where URLLC transmissions are scheduled. A heuristic

solution algorithm has been proposed to solve these problems jointly. Developing this optimization problem further in [29], the authors proposed an optimization-aided deep reinforcement learning (DRL) based framework, which included two phases, namely, eMBB resource allocation phase, and URLLC scheduling phase. The authors offered an approximate solution for resource allocation and validated their results using computer simulations. Differently from the abovementioned studies, the work in [30] considered the problem of minimizing the risk related to not meeting the URLLC deadline constraints. Specifically, the authors proposed a risk-sensitive approach for allocating resources to URLLC traffic and considered the conditional value at risk as the metric of interest. We specifically note that none of the abovementioned studies considered specifics of URLLC and eMBB traffic coexistence in industrial automation scenarios with complex blockage characteristics and potential for device-to-device offloading of URLLC transmissions.

The problem of isolation has also been studied in context of network slicing. The GSM Association in its NG.116 standard names slice isolation among the key expectations of network slicing [31]. In general, it must be addressed from at least three major perspectives: security, dependability and performance. Isolation in terms of security deals with not letting intentional attacks on one type of traffic affect the other traffic types, while dependability isolation relates to constraining fault propagation. A survey of existing, mostly security-motivated slice isolation techniques in the radio access network (RAN) and core networks can be found in [32] along with an approach to quantifying the isolation.

Performance isolation, which is the main focus of the present study, refers to minimizing the impact of congestion or workload upsurges in eMBB traffic on the performance of URLLC connections. The maximum possible performance isolation is provided by static resource reservation, where the capacities are strictly reserved for both eMBB and URLLC traffic and do not depend on the workload. However, such an approach may result in highly inefficient resource usage. Therefore, there is need for a dynamic policy that adapts resource for the current workload imposed by URLLC traffic.

B. OUR CONTRIBUTIONS

In this paper, we extend our efforts by considering a practical application of the priority-based traffic coexistence strategy. More specifically, we investigate the option of enabling the simultaneous support of eMBB and URLLC services via an explicit prioritization in industrial 5G NR deployments with dynamic blockage. For this purpose we join the tools of queuing theory and stochastic geometry to develop the framework simultaneously capturing propagation specifics as well as the service process at NR BS. Furthermore, to improve the system performance we also consider and compare three service strategy, where URLLC traffic might be offloaded onto direct D2D connections. In our study, we are interested in the density of NR BS required to provide a given performance guarantees to both traffic types. There guarantees are expressed in terms of URLLC and eMBB session drop probabilities.

The main contributions of our study are:

- the mathematical framework for assessment of the density of mmWave NR BSs in industrial environment with realistic dynamic blockage model and explicit prioritization of URLLC traffic and URLLC traffic offloading onto D2D connections;
- the priority-based implementation of URLLC and eMBB coexistence allows isolation of the former traffic efficiently and requires no external control during operation for all the considered strategies;
- it is vital to use BS-controlled D2D connectivity by reserving a fraction of resources for D2D traffic explicitly, as otherwise, interference dramatically diminishes the gains obtained by using D2D offloading strategy.

The rest of the paper is organized as follows. First, in Section II we provide an overview of the 5G use-cases and requirements for the industrial environment. We introduce the system model in Section III. The system is then analyzed in Sections IV, and V. Numerical results are presented in Section VI. Conclusions are drawn in the final section.

II. 5G IN INDUSTRIAL ENVIRONMENTS

In this section, we provide a perspective on wireless connectivity in the industrial environment. We start with describing the relevant wireless use-cases and then proceed highlighting NR technology's role in Industry 4.0.

A. INDUSTRY 4.0 CONCEPT

Following the market demands, the manufacturing industry undergoes continuous transformation (Fig. 1). Started as handicrafts manufacturing, it was delivering highly individual and expensive goods. Later technological revolutions targeted better productivity of manufacturing via the replacement of hand labor with machines. As a side effect of that process, products lost initial diversity and became standardized. This trend continued in the twentieth century, where the development of the manufacturing industry followed the paradigm of ''Fordism''. In social science, ''Fordism'' is defined as an economic system based on industrialized, *standardized mass production* and mass consumption [33].

Nowadays, the market demands higher individuality of products while retaining low prices and the stable quality of mass production. The paradigm of Fordism cannot address these new demands as manufacturing facilities are not flexible enough to accommodate frequent and rapid reconfigurations. Each reconfiguration of legacy manufacturing requires the development of new infrastructure, including communication systems that commonly rely on wired connections. The communication technologies and protocols used in legacy manufacturing are featured by high heterogeneity, which further complicates potential reconfigurations.

The ongoing industrial revolution, referred to as Industry 4.0, brings extensive automation and natively supported

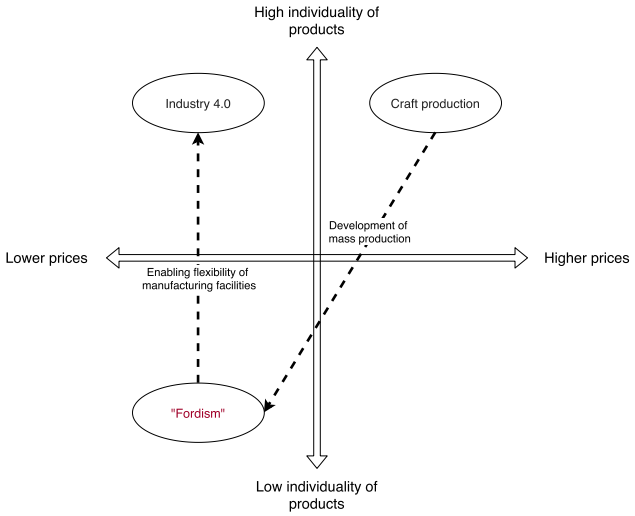

FIGURE 1. The evolution of the manufacturing process.

flexibility to manufacturing facilities. Such a transformation is driven by digitizing all physical systems and processes, creating unprecedented levels of awareness and knowledge. Effortless reconfiguration of manufacturing facilities further allows for adjusting to market demands dynamically by producing limited products with similar quality and cost compared to mass production.

Technologically speaking, manufacturing facilities in Industry 4.0 rely on the concept of Industrial IoT. Facilities on the floor consist of simple devices (sensors and actuators) capable of collecting data and performing a predefined set of actions. At the same time, factory intelligence controlling the floor resides in a cloud or on edge servers. Advanced wireless connectivity linked to this factory intelligence enables operational mobility for manufacturing machines. Such an architecture allows software-defined operation of the factories and on-demand reconfiguration of production lines.

B. WIRELESS CONNECTIVITY IN MANUFACTURING

According to 3GPP TS 22.104, the main applications areas of wireless technologies in manufacturing are: (i) replacing wired connections utilized in by legacy equipment, (ii) enabling motion control capabilities for mobile robotic platforms, (iii) control plane communications, (iv) monitoring of various goods and assets, (v) enabling human-machine interfaces. We consider each of these in detail below.

Wireless connectivity should replace legacy wired connections that currently dominate at the operational technology (OT) level (e.g., PROFINET, EtherCAT, Sercos, Modbus) [34]. This objective is significant for reducing costs at the early stage of the transformation of modern factories towards Industry 4.0. Legacy manufacturing machines, which can still be relevant to production, should be integrated into the emerging wireless deployment wherever possible. This can be enabled by embedding wireless UE into the machines.

The motion control systems is responsible for moving parts of machines. This process requires complex real-time communications between end devices (sensors and moving parts of machinery) and a motion controller. The motion control functionality can be supplemented with control-to-control communications enabling coordination between different machine controllers. The latter communications requirements are more relaxed as compared to motion control. However, control-to-control systems do not have a locked message structure and periodicity, leading to dynamically changing service demands.

The support of mobile robotic platform is critical for industrial automation on the factory floor. These devices may perform tasks such as transporting goods, materials, or other objects [35]. The mobile robots may demand network resources in different locations and require seamless handover when moving to ensure the QoS. The demanded latency and throughput may vary depending on the application. In challenging cases, such as the cooperative carrying of rigid or fragile objects in dynamically changing environments, the robotic system may require low latency and high throughput.

Assets and processes monitoring systems utilize sensor devices installed in the factory and provide information about ongoing operations. The diversity of sensors is not limited to simple measurements (e.g., temperature or pressure) and may utilize media control systems, such as regular or thermal video surveillance. Such media-based systems may notably contribute to the wireless network capacity demands.

Personnel is expected to still continue playing critical role even in further industrial deployments [36]. A wide set of interfaces can enable interaction between people and machines. Traditional control panels will evolve towards mobility support of maintenance personnel [37]. Furthermore, future factories are also expected to benefit from the use of virtual and augmented reality (VR/AR) technologies. These devices, that can be potentially built as head-mounted units with see-through displays, will enable additional assistance for workers on the factory floor further ensuring smooth and efficient human-machine interactions.

According to [36], the overall data flow in industrial deployments may reach several Gbps. The support of these rates inherently require wireless technologies characterized by extreme capacity such as NR operating in mmWave band. On the other hand, heterogeneous traffic demands of applications inherently call for explicit support at the air interface.

C. 5G NR IN FUTURE FACTORIES

The work on industrial use-cases in the context of 5G NR started in 3GPP Release 15. The use cases with strict latency requirements, including factory automation, are specified in Release 16. The scope of the ongoing standardization work is mainly on defining specific industrial demands that are not addressed by the current 5G NR technology state. Further releases will introduce enhancements into NR specifications.

From the perspective of a physical channel, the models listed in TR 38.901 currently do not include any industrial use-cases, which may have specifics affecting the

propagation conditions. Considering the manufacturing use-case, the physical channel may be significantly affected by dynamic blockage of mmWave links on the factory floor and electromagnetic interference caused by machinery. In addition to studies on the physical channel, radio resource management for industrial scenarios is also focused in the ongoing standardization work. This includes enabling Time-Sensitive Communication (TSC) services and handling resource management during aperiodic eMBB traffic peaks. TSC-related enhancements have to guarantee superior QoS as compared to wireless Ethernet, from UE to Core Network and backwards. The maximum end-to-end latency in such links should not exceed 1 ms, and the mean time between failures is ten years.

According to the 3GPP TS 22.104, in industrial scenarios, the TSC data rate may change dynamically and reach up to 500 Mbps. As TSC traffic peaks might overlap with eMBB peaks and cause a denial of service in the system, the dimensioning of 5G NR system in an industrial environment becomes crucial. In this paper, we investigate this question by considering URLLC and eMBB traffic coexistence strategies based on prioritization and D2D offloading mechanisms.

III. SYSTEM MODEL

In this section, we specify our system model. We start with the description of the considered scenario and then proceed with the wireless part and specifics for both considered traffic types with associated arrival processes and service procedures. Finally, we introduce the metrics of interest. Notations utilized in this paper are summarized in Table 1.

A. DEPLOYMENT

We consider a private 5G mmWave NR deployment in an industrial environment, i.e., a large autonomous factory with multiple production lines, as illustrated in Fig. 2(a). NR BSs are assumed to be installed on the ceiling at height h_A, where they organize a homogeneous Poisson point process (PPP) with density χ BS/m^2. These BSs produce circular coverage on the factory floor with radius r_N determined as shown in Fig. 2(a), which is determined based on the antenna and propagation model in Section IV. Each BS is assumed to operate by utilizing bandwidth W. We arbitrarily tag and consider a single NR BS.

The autonomous machines forming production lines are assumed to be located on the regular grid, see Fig. 2(b), with step size l meters, $l \ll r_N$. A machine's width and length are assumed to be equal and set to w, where $w/2 < l$. The latter condition ensures that machines do not overlap in space. To capture industrial environments with different densities of robotized equipment, we assume that each site contains an autonomous machine with probability ν.

We assume two types of UEs in our deployment. These are motion control devices, e.g., sensors or actuators, generating URLLC traffic and monitoring units, e.g., video cameras, generating eMBB traffic. The former are assumed to be located on autonomous machines on the factory floor. The monitoring units provide visual coverage of the factory floor, see Fig. 2. In our study, we consider uplink direction only assuming that uplink and downlink directions are separated by utilizing time-division duplex (TDD).

TABLE 1. Notation utilized in this paper.

Notation	Meaning
χ	Density of NR BSs
W	NR BS bandwidth
h_U	UE height
h_A	NR BS height
r_N	Radius of NR BS coverage area
SINR	Signal-to-noise plus interference ratio
P_U	UE transmit powers
G_U, G_A	UE and NR BS antenna arrray gains
N_0	Power spectral density of noise
L_B	Blockage losses
l	Grid step size
w	Width of a machine
ν	Probability of containing a machine at a grid point
κ	Probability of LoS path through machine
L	Path loss in linear scale
M_I	Interference margin
f_c	Carrier frequency
ζ	Propagation coefficient
α_H, α_V	HPBW in horizontal and vertical planes
G	Mean antenna gain
N	Number of antenna elements
λ_1	Arrival intensity of URLLC sessions
λ_2	Arrival intensity of eMBB sessions
μ_1^{-1}, μ_2^{-1}	Mean service time of URLLC and eMBB sessions
c_1	Rate of URLLC sessions
c_2^{min}	Minimum rate of eMBB sessions
D	Distance between two UEs
p_B	LoS path blockage probability
N_R	Maximum number of machines in the BS coverage
$b_{1,B}$	Resources required for URLLC session
$b_{1,D}$	Resources required for URLLC session in D2D mode
b_2^{min}	Minimum resources required for eMBB session
$r_{N,V}$	Distance between NR BSs
$r_{N,S}$	Maximum coverage of a NR BS
S_{th}	SINR corresponding to the lowest feasible NR MCS
$E[S_{e,B}]$	Mean spectral efficiency of UE to BS link
$E[S_{e,D}]$	Mean spectral efficiency of a D2D link
B	Overall amount of resources for uplink NR BS interface
Δ	Mean amount of resources utilized by D2D links
p_I	Probability of interference
$p_{I,T}$	Interference probability in frequency-time
$p_{I,S}$	Interference probability in space
F_0	Area of NR BS coverage
F_1	Area of D2D interference zone
F_2	Area of NR BS to UE interference zone
L_0	Perimeter of NR BS coverage
L_1	Perimeter of D2D interference zone
L_2	Perimeter of NR BS to UE interference zone
W_0	Distance between UE and the center of cell
$p_{L,U}$	URLLC session drop probability
$p_{L,U}^*$	Overall URLLC session drop probability
N_1	Maximum number of URLLC sessions
N_2	Maximum number of eMBB sessions
$\mathbf{X}$	State-space of the CTMC
$\mathbf{p}$	Stationary state probability distribution
$\mathbf{A}$	Infinitesimal generator matrix
p_{B_1}	URLLC session drop probability
p_{B_2}	eMBB session drop probability
p_{pre}	eMBB session preemption probability
U	Resource utilization

B. BLOCKAGE MODEL

We assume that autonomous machines act as blockers to mmWave propagation. Note that mmWave propagation

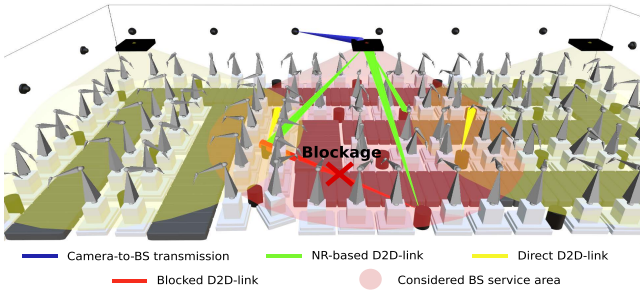

(a) 5G mmWave factory deployment

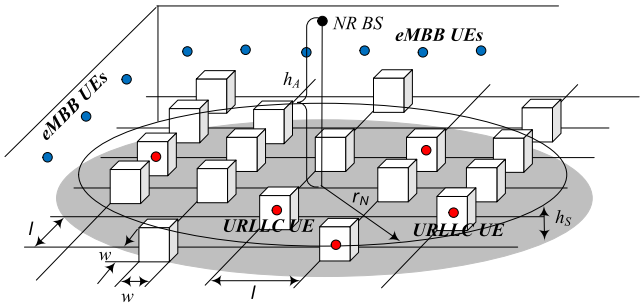

(b) Geometric model

FIGURE 2. Illustration of the considered scenario.

industrial environment blockage is more complicated than human blockage and building blockage models [38]–[40]. The rationale is that the latter can be assumed to be homogeneous attenuating mmWave signal equally at different instants of time. Differently, as robotized machines often perform jobs utilizing moving hands, their blockage is non-uniform in time. Fig. 2 demonstrates the heat map characterizing the attenuation of a typical automatic hand averaged over time. Thus, in this paper, we assume that each autonomous machine is characterized with a constant permeability for mmWave signal. In other words, at any arbitrarily chosen instant of time, there exists a propagation path through the robotized equipment with probability κ. One can determine this coefficient utilizing the photometric approach from [41].

C. PROPAGATION MODEL

The signal-to-noise plus interference ratio (SINR) at the receiver can be written in the following form

$$S(y) = \frac{P_U G_A G_U}{L(y)(N_0 W + M_I)}, \tag{1}$$

where y is the distance between receiver and NR BS, P_U is the transmit power at UE, G_A and G_U are the NR BS and UE antenna array gains, N_0 is the thermal noise power, W is the utilized bandwidth, $L(y)$ is the path loss, M_I is the interference margin. Note that the interference between adjacent BSs in the environment is captured by the constant interference margin, M_I. In practice, one may estimate M_I using the models proposed in the literature [42], [43].

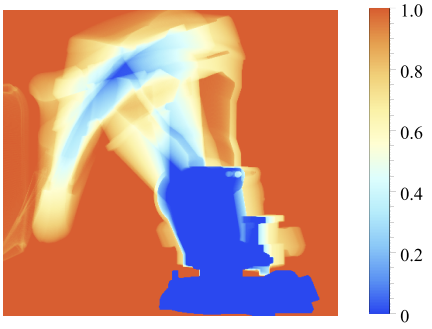

FIGURE 3. Non-homogeneous attenuation by moving autonomous hand.

By following [44], the path loss can be written as

$$L_{dB}(y) = 32.4 + 21 \log_{10} y + 20 \log_{10} f_c, \tag{2}$$

where f_c is the frequency and y is the distance between communicating entities. Note that blockage is assumed to cause additional loss of L_B. In what follows, we utilize the linear scale by using the model in the form $Ay^{-\zeta}$, where ζ is the path loss exponent, A is the propagation coefficient that can be estimated from (2) as

$$A = 10^{2 \log_{10} f_c + 3.24}, \ \zeta = 2.1. \tag{3}$$

Finally, SINR is written as follows

$$S(y) = Hy^{-\zeta}, \ H = P_U G_A G_U / A(N_0 W + M_I). \tag{4}$$

D. ANTENNA MODEL

At UE and NR BS sides we assume $N_U \times N_U$ and $N_A \times N_A$ planar antenna arrays. To model their radiation patterns, we consider a pyramidal antenna model. According to it, the radiation pattern is defined by two angles, α_H and α_V capturing directivity of antenna arrays in horizontal and vertical planes coinciding with HPBWs of the antenna radiation patterns. Note that α_H and α_V are proportional to the number of antenna elements as [45]

$$\alpha = 2|\theta_m - \theta_{3db}|, \tag{5}$$

where θ_m is the array maximum, θ_{3db} is the 3dB angle.

The gain over the HPBW in the appropriate plane, $G_{(\cdot)}$ can be found as [45]

$$G_{(\cdot)} = \frac{1}{\theta^+_{3db} - \theta^-_{3db}} \int_{\theta^-_{3db}}^{\theta^+_{3db}} \frac{\sin(N_{(\cdot)} \pi \cos(\theta)/2)}{\sin(\pi \cos(\theta)/2)} d\theta, \tag{6}$$

where the upper and the lower 3-dB points are

$$\theta^{\pm}_{3db} = \arccos[-\beta \pm 2.782/(N\pi)], \tag{7}$$

and $N_{(\cdot)}$ is the number of antenna elements. The overall antenna gains at UE and NR BS sides are obtained as $G_A = G_{A,V} G_{A,H}$ and $G_U = G_{U,V} G_{U,H}$.

E. TRAFFIC, PRIORITIES, AND SERVICE STRATEGIES

Monitoring sessions are assumed to arrive according to homogeneous Poisson process with intensity λ_2. The traffic is assumed to be elastic with the minimum rate requirement $c_2^{\min}$, $c_2^{\min} \geq 1$. The actual resource requirements may vary depending on the UE location. The service time distribution is exponential with intensity μ_2. URLLC sensor traffic arrives according to homogeneous Poisson process with intensity λ_1. These sessions require constant rate, c_1, $c_1 \geq 1$. Similarly to eMBB sessions, the actual amount of requested resources may vary depending on the location of UE and the utilized service strategy defined below. The service time distribution is exponential with intensity μ_1.

We assume the preemptive priority service discipline. According to it, URLLC sensor sessions are assumed to have absolute priority over eMBB monitoring sessions. In other words, the former traffic has exclusive access to resources and may interrupt ongoing service of eMBB sessions. Note that eMBB sessions can be lost at the moment of arrival when there are no sufficient amount of resources available to provide the requested rate $c_2^{\min}$. Alternatively, they can also be lost during the ongoing service if the provided rate falls below this value. The loss of URLLC sessions may only happen at the moment of arrival when all the resources are occupied by URLLC traffic.

We consider the following three service strategies:

- *Baseline.* According to this strategy, URLLC and eMBB traffic is transmitted over NR BS. In this case, both traffic types are bottlenecked at the uplink NR slot, limiting system performance.
- *D2D-aware.* In this strategy, attempting to minimize the load in the uplink direction, we enable NR-based D2D communications for URLLC traffic, allowing sensors, actuators, and monitoring units to communicate directly whenever possible. NR BS is assumed to schedule D2D transmissions by reserving a fraction of resources. In this strategy, no additional interference is created by D2D transmissions, but the amount of resources remaining to serve eMBB and URLLC traffic that cannot be offloaded to direct links reduces. Despite utilizing D2D links, the scheduling is performed centrally at NR BS.
- *D2D-unaware.* In this strategy, URLLC traffic can still be offloaded to D2D links, but the scheduling process at NR BS is omitted. Sensors, actuators, and monitoring units are allowed to utilize D2D links without any prior coordination. This strategy may effectively reduce the delay for URLLC transmission, but uncoordinated operation induces interference reducing the reliability.

F. METRICS OF INTEREST AND APPROACH

The ultimate measure of interest in this paper is the density of NR BSs required for fulfilling the prescribed key performance indicators (KPIs) in each of the considered service strategies for a given intensity of both traffic types. The metrics used in the assessment include session drop probabilities of both traffic types as well as eMBB session preemption probability. We derive the latter as a function of system parameters and then conclude the required density of NR BS in the considered environment.

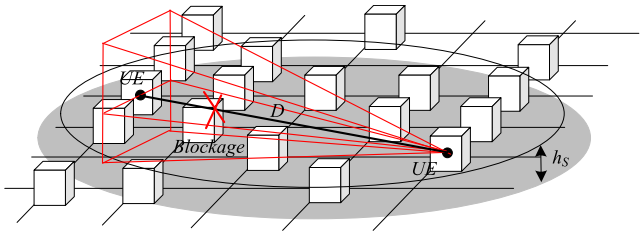

FIGURE 4. Illustration of blockage in the industrial environment.

The methodology developed in this paper can be logically divided into two parts: (i) characterization of radio part specifics and (ii) queuing model formalization and analysis. The former stage accounts for specifics of the considered service strategies providing parameters of interest for the second stage. At the second stage, a queuing system with preemptive priority discipline capturing the details of the traffic coexistence is developed. This queuing framework is unified for all the considered strategies, and depending on input parameters determined at the first stage, delivers the abovementioned KPIs.

IV. TRAFFIC SERVICE STRATEGIES

In this section, we analyze the service strategies introduced in the previous chapter. Based on performed analysis, we further parameterize NR BS service process, including the arrival processes of URLLC and eMBB sessions and the amount of resources at NR BS.

A. BLOCKAGE PROCESS

To determine the amount of URLLC traffic that can be offloaded to D2D links, one has to derive the probability that a LoS path between two URLLC UEs is available, see Fig. 4. Recalling our assumption that the grid size is much smaller than the coverage radius of the NR BS, $l \ll R$, we observe that the distance between two randomly chosen UEs, D, can be approximated by the distance between two uniformly distributed points in a circle that obeys the following probability density function (pdf) [46]

$$f_D(x) = \frac{2x}{r_N^2}\left[\frac{2}{\pi}\cos^{-1}\left(\frac{x}{2r_N}\right) - \frac{x}{r_N\pi}\sqrt{1-\frac{x^2}{4r_N^2}}\right], \quad (8)$$

where r_N is the coverage of NR BS provided in the following section. This approximation becomes better as $l \to 0$.

Let us now fix a certain distance between two URLLC UEs, x. To determine the blockage probability of a LoS path we need to obtain the probability mass function (pmf) of the number of autonomous machines it crosses. Note that while the direct probabilistic derivation of this pmf is feasible, it leads to unnecessary complexity. To this aim, we utilize the methods of integral geometry [47] that has been recently utilized to tackle various complex problems

in cellular networking [48], [49]. According to [50], the probability that a segment of a line S (LoS path between considered UEs) and convex region K (machine's projection on xOy plane) both randomly dropped into another convex region K_0 (NR BS coverage area) intersect is given by

$$p_{B,1}(x) = \frac{m(S; S \cap K \neq \emptyset)}{m(S \subset K_0)}, \tag{9}$$

where $m(S; S \cap K \neq \emptyset)$ is the kinematic density of all motions of S and K such that S intersects K, $m(S \subset K_0)$ is the kinematic density of motions of S such that it is in K_0.

The nominator in (10) is given by [50]

$$m(S; S \cap K \neq \emptyset) = 2\pi F + 2xL, \tag{10}$$

where $F = w^2$ and $L = 4w$ are the square and perimeter of K, x is the length of the segment. The density $m(S \subset K_0)$ can be obtained in special cases of region K_0. In our case K_0 is a circle with radius r_N, and thus, we have [50]

$$m(S \subset K_0) = \frac{1}{2}\pi\Big(4\pi r_N^2 - 8r_N^2 \sin^{-1}(x/2r_N) - \\ -2x\sqrt{4r_N^2 - x^2}\Big). \tag{11}$$

Combining these results, the probability that the LoS path between two UEs crosses a single machine is given by

$$p_{B,1}(x) \\ = \frac{2w(\pi w + 4x)}{\pi(2\pi r_N^2 - 4r_N^2 \sin^{-1}(x/2r_N) - x\sqrt{4r_N^2 - x^2})} \times (1-\kappa), \tag{12}$$

where κ is the probability of a LoS path through the machine.

Observe that there might be more than a single autonomous machine intersecting the LoS path. According to our model, the maximum number of autonomous machines, N_R, contained in the NR BS coverage can be found directly or utilizing one of the approximations to the Gauss circle problem [51]. Thus, the overall number of machines follows Binomial distribution with parameters N_R and ν, where the latter is the probability that a site contains a machine.

Now, the probability that a LoS path is blocked is

$$p_B(x) = \sum_{i=1}^{N_R} \binom{N_R}{i} \nu^i (1-\nu)^{N_R - i} \\ \times [1 - (1 - p_{B,1}(x))]^i. \tag{13}$$

Finally, the sought blockage probability is obtained as

$$p_B = \int_0^{2r_N} f_D(x) p_B(x) dx. \tag{14}$$

Recall that for *baseline* strategy all URLLC UEs are served utilizing a NR BS. For the rest of the strategies, the URLLC traffic intensity arriving at a NR BS is given by $p_B\lambda_1$, while $(1 - p_B)\lambda_1$ is served via D2D links.

B. SESSION RESOURCE REQUIREMENTS

Observe that in spite of the constant bit rate required by URLLC sessions, c_1, $c_1 \geq 1$, and the minimum rate needed by eMBB monitoring sessions, $c_2^{\min}$, $c_2^{\min} \geq 1$, the actual amount of requested resource, $b_2^{\min}$ and $b_{1,B}$, may vary due to random geometric locations of UEs. On top of this, we also need to determine the amount of resources required when URLLC UE utilizes a D2D link, $b_{1,D}$. These quantities depend on the coverage of the considered NR BS. In this section, we thus first proceed by obtaining the coverage radius of NR BS, r_N. By recalling our deployment assumptions, we see that the latter is affected by both the maximum coverage of NR BS $r_{N,S}$ and the distance between NR BSs, whichever smaller, i.e., $r_N = \min(r_{N,S}, r_{N,V})$.

Observe that the the radius $r_{N,S}$ characterized the maximum distance between UE and NR BS such that there is no outage in blocked conditions. By utilizing the propagation model, the SINR at the distance $r_{N,S}$ is given by

$$S = H\left(r_{N,S}^2 + (h_A - h_U)^2\right)^{-\frac{\zeta}{2}} / L_B = S_{th}, \tag{15}$$

where L_B is the blockage induced attenuation, S_{th} is the SINR that corresponds to the lowest NR MCS [18]. Solving (15) with respect for r_N, we have

$$r_{N,S} = \sqrt{(H/L_B S_{th})^{\frac{2}{\zeta}} - (h_A - h_U)^2}. \tag{16}$$

Observe that the value of H in (4) directly affects $r_{N,S}$. The latter is further affected by the antenna radiation pattern parameters in (5)–(6). In this paper, we approximate $r_{N,V}$ by the circle having the same area as the Voronoi cells induces by the PPP deployment of NR BSs. To this aim, we utilize computer simulation techniques to obtain the area of the Voronoi cell for a given density of NR BSs, χ BS/m^2.

Once radii $r_{N,V}$ and $r_{N,S}$ are obtained, one may characterize the required resources, b_2^{min} and b_1. Recalling that UEs are uniformly distributed in the coverage of NR BS, the mean spectral efficiency can be obtained as follows

$$E[S_{e,B}] = \int_0^{r_N} \frac{2x}{r_N} \log_2[1 + S(y)] dx, \tag{17}$$

where $S(y)$ is defined in (4), while for D2D links we have

$$E[S_{e,D}] = \int_0^{2r_N} f_D(x) \log_2[1 + S(y)] dx, \tag{18}$$

where $f_D(x)$ is provided in (8).

By utilizing the rate required by URLLC sessions, c_1, $c_1 \geq 1$, and the minimum rate needed by eMBB monitoring sessions, $c_2^{\min}$, $c_2^{\min} \geq 1$, we now utilize the mean spectral efficiency to estimate the mean amount of resources requested by considered UEs as follows

$$b_2^{\min} = c_2^{\min}/E[S_{e,B}], \\ b_{1,B} = c_1/E[S_{e,B}], \\ b_{1,D} = c_1/E[S_{e,D}]. \tag{19}$$

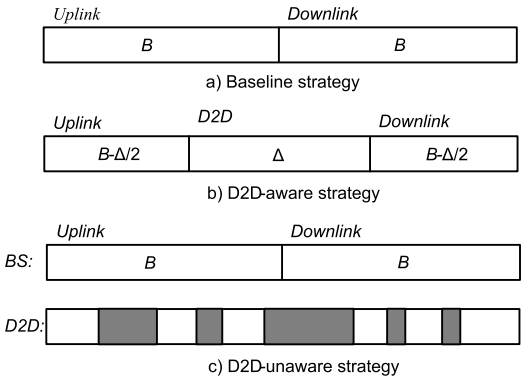

FIGURE 5. Illustration of resource allocations in the considered strategies.

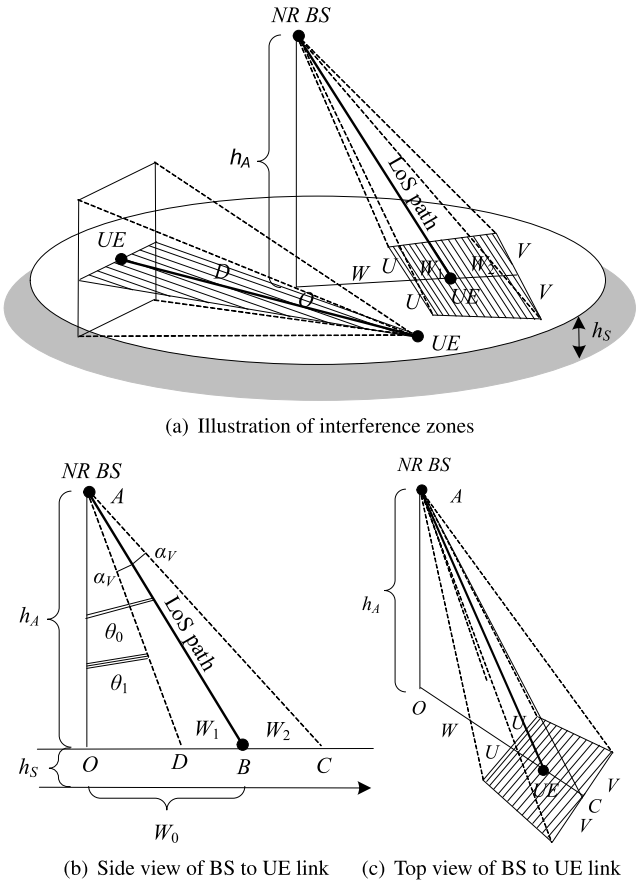

FIGURE 6. Illustration of spatial interference in ***D2D-unaware*** strategy.

By utilizing the employed NR numerology the mean amount of requested resources are further converted into primary resource blocks (PRB).

C. SPECIFICS OF D2D OFFLOADING STRATEGIES

1) D2D-AWARE STRATEGY

Recall, that in the baseline strategy, all the uplink NR resources are devoted to the serving of URLLC and eMBB sessions with arrival intensities λ_1 and λ_2. For the D2D-aware strategy, not only the arrival intensity of URLLC sessions reduces to $p_B\lambda_1$, but the amount of resources available in the uplink direction decreases as well, see Fig. 5. To quantify this reduction, we utilize the mean spectral efficiency of the D2D links provided in (18) leading to the mean overall amount of resources utilized by D2D links in the following form

$$\Delta = \lambda_1(1-p_B)\frac{c_1}{E[S_{e,D}]}, \tag{20}$$

while the rate left for uplink NR BS interface is then $B-\Delta/2$.

2) D2D-UNAWARE STRATEGY

Differently from *D2D-aware* strategy, the utilization of the D2D links does not directly reduce the number of resources available in the uplink direction as the NR BS does not schedule these transmissions. Instead, they may induce interference negatively affecting the reception of URLLC data, see Fig. 5. Observing that due to the utilization of directional antennas at a UE and a NR BS and accounting for the fact that the NR BS height is higher than the UE height, the interference in the uplink direction is negligible. The main effect of interference is observed in the downlink direction, where overlapping beams may lead to the loss of URLLC data transmitted over D2D connections.

Observe that downlink NR BS to UE URLLC transmission interferes with direct D2D URLLC transmission if they coincide in time and space. Since these two events are independent, we may write $p_I = p_{I,T}p_{I,S}$, where $p_{I,T}$ and $p_{I,S}$ are interference probabilities in time and space, respectively. Since D2D transmission in the considered *D2D-unaware* strategy may start at any instant of time and occupy a randomly chosen subcarrier, the former is immediately given by $p_{I,T} = \min(\Delta, 2B)/2B$, where $2B$ is the overall resource available in uplink and downlink directions, see Fig. 5. We now proceed with the latter probability.

We first determine the probability that the downlink transmission to the UE overlaps with the D2D transmission. To this aim, we again utilize the integral geometry, see Fig. 6. By following [50], the probability that an arbitrarily chosen D2D transmission interferes with arbitrarily chosen downlink URLLC transmission can be approximated by

$$p_{I,S} = \frac{2\pi(F_1+F_2)+L_1L_2}{2\pi(F_0+F_2)+L_0L_2}, \tag{21}$$

where F_0, F_1, and F_2 are the areas of NR BS coverage, interference zone associated with D2D transmission and interference zone associated with downlink NR BS to UE transmission, respectively, while L_0, L_1, and L_2 are perimeters.

To determine the sought probability, we need to obtained all the unknowns in (21). Note that $F_0 = \pi r_N^2$, $L_0 = 2\pi r_N$. Observing Fig. 6 one may notice that the interference zone associated with D2D transmission is characterized by a triangular form while the one associated with NR BS to UE transmission is of trapezoidal form. We immediately see that $F_1 = DL/2 = D^2(\tan\alpha_H/2)$, where α_H is the HPBW in a horizontal plane, D is the distance between communicating

UEs determined in (8), while the perimeter is given by

$$L_1 = 2\sqrt{D^2 + (D\tan(\alpha_H/2))^2} + 2D\tan(\alpha_H/2). \quad (22)$$

By utilizing the law of the unconscious statistician, the mean area and perimeter are given by

$$E[F_1] = \int_0^{2r_N} x^2 \tan(\alpha_H/2) f_D(x)dx,$$
$$E[L_1] = \int_0^{2r_N} L_1(x) f_D(x)dx, \quad (23)$$

where r_N is the radius of NR BS coverage.

Consider now the downlink NR BS to UE direction. To determine the interference zone's area and perimeter, we first need to obtain the height and base lengths. By analyzing Fig. 6(b) we observe that $\tan\theta_0 = W_0/h_A$, where W_0 is the distance to the center of the cell. Thus, $\theta_1 = \theta_0 - \alpha_V = \tan^{-1}(W_0/h_A) - \alpha_V$. By utilizing $\tan\theta_1 = (W_0 - W_1)/h_A$ we may write

$$W_1 = W_0 - h_A \tan\left(\tan^{-1}\frac{W_0}{h_A} - \alpha_V\right). \quad (24)$$

Similarly we have for W_2

$$W_2 = h_A \tan\left(\tan^{-1}\frac{W_0}{h_A} + \alpha_V\right) - W_0. \quad (25)$$

The base length can be found utilizing right triangles in Fig. 6(c). Particularly, since

$$||AC|| = \sqrt{h_A^2 + (W_0 + W_2)^2},$$
$$||AD|| = \sqrt{h_A^2 + (W_0 - W_1)^2}, \quad (26)$$

we obtain

$$V = \tan(\alpha_H/2)\sqrt{h_A^2 + (W_0 + W_2)^2}$$
$$U = \tan(\alpha_H/2)\sqrt{h_A^2 + (W_0 - W_1)^2}, \quad (27)$$

leading to the following

$$F_2 = \frac{1}{2}(2V + 2U)(W_1 + W_2). \quad (28)$$

The only parameter left to determine is a side of a trapezoid which directly stems from the Fig. 6(b) and Fig. 6(c). Finally, we have for the perimeter

$$L_2 = 2U + 2V + 2\sqrt{(W_1 + W_2)^2 + (V - U)^2}. \quad (29)$$

Now, the mean square and perimeter are determined similarly to $E[F_1]$ and $E[L_1]$ by utilizing the law of the unconscious statistician with pdf $f_W(x) = 2x/r_N^2$, i.e.,

$$E[F_2] = \int_0^{r_N} f_W(x)F_2(x)dx,$$
$$E[L_2] = \int_0^{r_N} f_W(x)L_2(x)dx, \quad (30)$$

where r_N is the radius of the BS coverage zone.

Thus, the overall URLLC session loss probability reads as

$$p^{\star}_{L,U} = (1 - p_B)p_I + p_B[1 - (1 - p_{L,U})(1 - p_I)], \quad (31)$$

where p_B is the probability of utilizing UE to NR BS interface for URLLC data transmission, p_I is the probability of interference, $p_{L,U}$ is the probability that URLLC session is dropped at NR BS due to insufficient amount of resources available. The latter parameter is derived in the next section.

V. QUEUING FORMALIZATION

In this this section, we formalize the queuing system describing the service process of URLLC and eMBB traffic with preemptive-priority discipline. We then solve it by utilizing the embedded Markov chain approach and, finally, estimate the session drop and preemption probabilities.

A. QUEUING MODEL

We are now in position to formulate the queuing model describing the service process of NR BS. The system of interest can be modeled as a queuing system with two Poisson arrival processes, exponentially distributed services time and preemptive priority service. The behavior of this queuing system can be described by the two-dimensional continuous-time Markov chain (CTMC) $X(t) = (N_1(t), N_2(t)), t > 0$, where $N_1(t)$ represents the number of high-priority URLLC sessions in the system at time t, $N_2(t)$ captures the number of lower priority eMBB sessions at time t. The considered process is defined over the following state space

$$X = \{(n_1, n_2) : n_1 \geq 0, n_2 \geq 0, \quad n_1 b_1 + n_2 b_2^{\min} \leq C\}, \quad (32)$$

where n_1 is the number of URLLC sessions, n_2 is the number of eMBB sessions that are currently in the system.

In order to proceed we need the following notation. Let $N_1 = \lfloor C/b_1 \rfloor$ and $N_2 = \lfloor C/b_2^{\min} \rfloor$ be the maximum number of URLLC and eMBB sessions currently in service. Further, we denote by $k(n_1) = \lfloor C - n_1 b_1/b_2^{\min} \rfloor$ the maximum number of lower priority eMBB sessions in the system when the number of URLLC sessions in service is exactly n_1. Recalling that the eMBB traffic is assumed to be elastic in nature, the amount of resources available to these sessions in the system is equally distributed between them and depends on the current state $(n_1, n_2) \in X$. That is, we have

$$b_2(n_1, n_2) = \left\lfloor \frac{C - n_1 b_1}{n_2} \right\rfloor \geq b_2^{\min}. \quad (33)$$

Consider now the process of eMBB and URLLC traffic admission to the system. Particularly, when a new URLLC session arrives to the system the following may happen:

- if upon arrival of the new session there are more than b_1 PRBs available, this session is accepted to the system without any consequences for eMBB sessions;
- if (i) the arriving session observes less than b_1 free PRBs in the system and, (ii) the current amount of URLLC sessions in service is smaller than N_1, and (iii) there are more than 0 eMBB sessions currently in service, URLLC session is admitted to the system causing the preemption of $\lceil (b_1 - C + (n_1 b_1 + n_2 b_2^{\min}))/b_2^{\min} \rceil$ lower priority eMBB sessions;

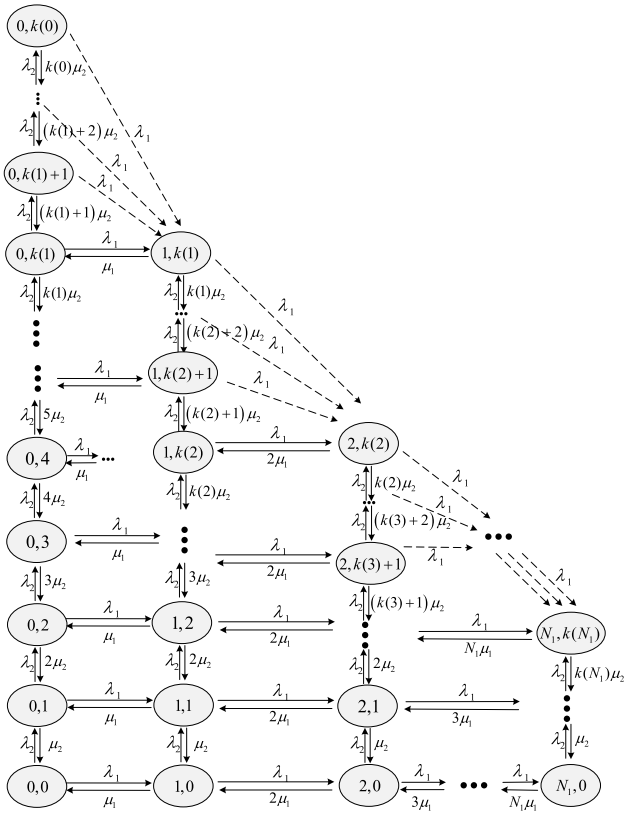

FIGURE 7. The general view of the state transition diagram.

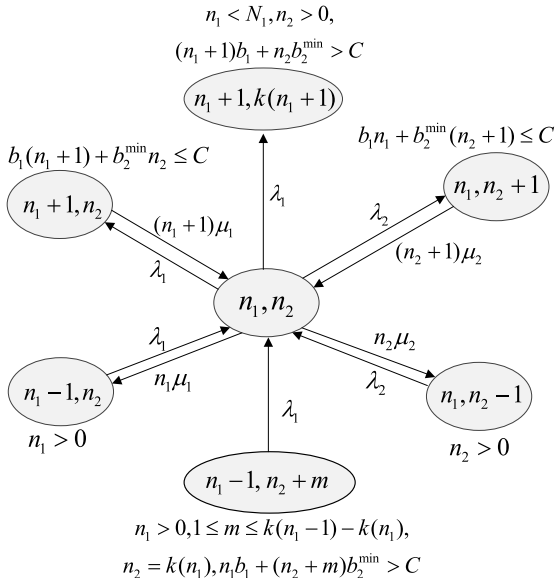

FIGURE 8. Transition probabilities of the central state of the model.

- of none of the above happens, the session is rejected.

Consider now the arrival of eMBB session. We have:

- if the state number of free PRBs at the moment of arrival is higher than, $b_2(n_1, n_2)$ the session is accepted for service and allocated $b_2(n_1, n_2)$ PRBs;
- in any other case, the session is dropped.

By utilizing the rules specified above we can fully characterize the stochastic process $X(t)$ describing the service of URLLC and eMBB sessions. Specifically, the state transition diagram of the whole process is shown in Fig. 7 while Fig. 8 highlights details of arbitrarily chosen ''central'' state of the process. Since the capacity of the system is limited, the process $X(t)$ is ergodic and we can utilize the local balance principle to derive equations characterizing $X(t)$ in equilibrium conditions, see (35), as shown at the bottom of the next page, for $n_1 = 0, 1, \ldots, N_1$ and $n_2 = 0, 1, \ldots, N_2$, where we use the following shortcut

$$\left\lceil \frac{b_1 - C + (n_1 b_1 + n_2 b_2^{\min})}{b_2^{\min}} \right\rceil = q(n_1, n_2). \tag{34}$$

Denote by $\{p(n_1, n_2), (n_1, n_2) \in X\} = p$ the steady-state probability distribution of the queuing system $X(t)$. Observe that the underlying Markov chain is not reversible meaning that there is no closed-form solution for p. Nevertheless, the steady-state distribution can be estimated numerically by solving the following set of linear equations

$$pA = 0, p1^T = 1, \tag{37}$$

where $\mathbf{A}$ is infinitesimal generator constituting of elements $a((n_1, n_2), (n_1', n_2'))$ defined in (36), as shown at the bottom of the next page, with the shorthand

$$\begin{aligned} * = &-[\lambda_1 I\{n_1 < N_1, b_1(n_1+1) + b_2^{\min} n_2 \le C\} \\ &+ \lambda_1 I\{n_1 < N_1, n_2 > 0, b_1(n_1+1) + b_2^{\min} n_2 > C\} \\ &+ \lambda_2 I\{n_2 < N_2, b_1 n_1 + b_2^{\min}(n_2+1) \le C\} \\ &+ n_1\mu_1 + n_2\mu_2]. \end{aligned} \tag{38}$$

Once the steady-state distribution p is found, we may proceed determining the performance measures of the system:

- drop probability of URLLC session is given by

$$p_{B_1} = \sum_{i=0}^{k(N_1)} p(N_1, i); \tag{39}$$

- drop probability of eMBB session is provided as

$$p_{B_2} = \sum_{i=0}^{N_1} p(i, k(i)); \tag{40}$$

- the preemption probability of eMBB session, p_{pre}, that is, the probability that an arbitrarily chosen eMBB session is dropped during ongoing service

$$p_{pre} = \sum_{i=0}^{N_1-1} \sum_{\substack{j=k(i+1)+1 \\ k(i)\neq k(i+1)}}^{k(i)} \frac{\lambda_1 p(i,j)}{\lambda_1 + \lambda_2 I\{j < k(i)\} + i\mu_1 + j\mu_2}; \tag{41}$$

- the fraction of utilized resources, U, is provided as

$$U = C \sum_{i=0}^{N_1} \sum_{j=1}^{k(i)} p(i,j) + b_1 \sum_{i=1}^{N_1} i p(i,0). \tag{42}$$

VI. NUMERICAL RESULTS

In this section, we report our numerical results. We start characterizing the fraction of URLLC traffic that can be offloaded onto D2D connections as a function of environmental parameters. Then, we proceed with characterizing the trade-offs associated with the considered strategies. Here, we utilize the URLLC and eMBB session drop probabilities and eMBB session preemption probability as the main metrics of interest. These dependencies can then be used to determine the density of NR BSs to maintain the required level of system performance. To this end, we finally report the sample density of BSs to be installed to maintain the desired level of URLLC and eMBB traffic metrics.

The default system and environmental parameters utilized for computing the numerical results are provided in Table 2. We specifically note that we set the mean service time of URLLC sessions to exactly 1 ms, i.e., $\mu_1 = 10^3$. Also, to guarantee the reliable delivery of URLLC data, we assume repetition coding implying that six replicas of the same URLLC packet are sent during the session. According to this procedure and assuming a single packet payload of 20 bytes, the resulting size of the payload of a single URLLC session is 120 bytes.

TABLE 2. Parameters utilized for numerical assessment.

Parameter	Value
Carrier frequency	28 GHz
NR BS bandwidth	50 MHz
Transmit power	0.2 W
Power spectral density of noise	-174 dBm
SINR corresponding to the lowest NR MCS	-8.7 dBm
Interference margin	3 dB
Propagation exponent	2.1
Default of NR BSs density	10^{-4} $1/\text{m}^2$
NR BS antenna array	8x4, 16x4, 32x4
UE antenna array	4x4, 16x4
NR BS and UE heights	10 m, 1.7 m
Blockage induced attenuation	20 dB
NR numerology	3
Arrival intensity of URLLC sessions	5000 sess./s
Arrival intensity of eMBB sessions	100 sess./s
Mean service time of URLLC sessions	1 ms
Mean service time of eMBB sessions	120 s
URLLC session payload	120 bytes
Number of repetitions for URLLC message	6
Minimum rate of eMBB sessions	1 Mbps
Grid step size	15 m
Width of machine	$l/3$ m
Probability of containing machine at a grid point	0.5
Probability of LoS path through machine	0.1

A. OFFLOADING CHARACTERIZATION

We start considering the intensity of URLLC sessions that can be offloaded onto D2D connections as a function of environmental characteristics. To this end, Fig. 9 illustrates the URLLC D2D intensity obtained as $\Lambda_S = \lambda_1(1 - p_B)$, where p_B is the probability that a LoS path between two UEs is not occluded derived in (14) as a function of geometric deployment parameters including grid size l, probability of having a LoS path through the machine, κ, and probability of having a machine at a lattice point, ν.

Analyzing the presented data, one may observe that, logically, the D2D traffic intensity increases when the grid step size gets larger while the rest of the environmental parameters are kept constant. Nevertheless, even for a relatively high machine density on the factory floor with $l = 10$ m, $\nu = 0.8$, and $\kappa = 0.1$ a significant part of URLLC traffic can be potentially offloaded onto D2D connections. The effect of machine "transparency" is more profound, as indicated in Fig. 9(b). Here, a faster-than-linear increase in the intensity is explained by the associated decrease in the blockage probability. Thus, the linear increase in machine "transparency" leads to faster growth in the LoS probability.

$$
\begin{aligned}
&[\lambda_1 I\{n_1 < N_1, b_1(n_1+1) + b_2^{\min} n_2 \le C\} + \lambda_2 I\{n_2 < N_2, b_1 n_1 + b_2^{\min}(n_2+1) \le C\} + n_1\mu_1 + n_2\mu_2 + \\
&\quad + \lambda_1 I\{n_1 < N_1, n_2 > 0, b_1(n_1+1) + b_2^{\min} n_2 > C\}]p(n_1, n_2) = \lambda_1 I\{n_1 > 0, b_1 n_1 + b_2^{\min} n_2 \le C\}p(n_1-1, n_2) + \\
&\quad + \lambda_2 I\{n_2 > 0, b_1 n_1 + b_2^{\min} n_2 \le C\}p(n_1, n_2-1) + (n_1+1)\mu_1 I\{n_1 < N_1, b_1(n_1+1) + b_2^{\min} n_2 \le C\}p(n_1+1, n_2) + \\
&\quad + (n_2+1)\mu_2 I\{n_2 < N_2, b_1 n_1 + b_2^{\min}(n_2+1) \le C\}p(n_1, n_2+1) + \\
&\quad + \lambda_1 I\{n_1 > 0, n_2+1 \le N_2, b_1(n_1-1) + b_2^{\min}(n_2+1) \le C, b_1 n_1 + b_2^{\min}(n_2+1) > C\}p(n_1-1, n_2+1) + \ldots + \\
&\quad + \lambda_1 I\{n_1 > 0, b_1(n_1-1) + b_2^{\min} k(n_1-1) \le C, b_1 n_1 + b_2^{\min} k(n_1-1) > C\}p(n_1-1, k(n_1-1))
\end{aligned} \tag{35}
$$

$$
a((n_1, n_2), (n_1', n_2')) = \begin{cases}
\lambda_1, & \text{if } n_1' = n_1+1, n_2' = n_2, n_1 < N_1, b_1(n_1+1) + b_2^{\min} n_2 \le C, \\
& \text{or } n_1' = n_1+1, n_2' = n_2 - q(n_1, n_2), n_1 < N_1, n_2 > 0, b_1(n_1+1) + b_2^{\min} n_2 > C; \\
\lambda_2, & \text{if } n_1' = n_1, n_2' = n_2+1, n_2 < N_2, b_1 n_1 + b_2^{\min}(n_2+1) \le C; \\
n_1\mu_1, & \text{if } n_1' = n_1-1, n_2' = n_2, n_1 > 0; \\
n_2\mu_2, & \text{if } n_1' = n_1, n_2' = n_2-1, n_2 > 0; \\
*, & \text{if } n_1' = n_1, n_2' = n_2; \\
0, & \text{otherwise}
\end{cases} \tag{36}
$$

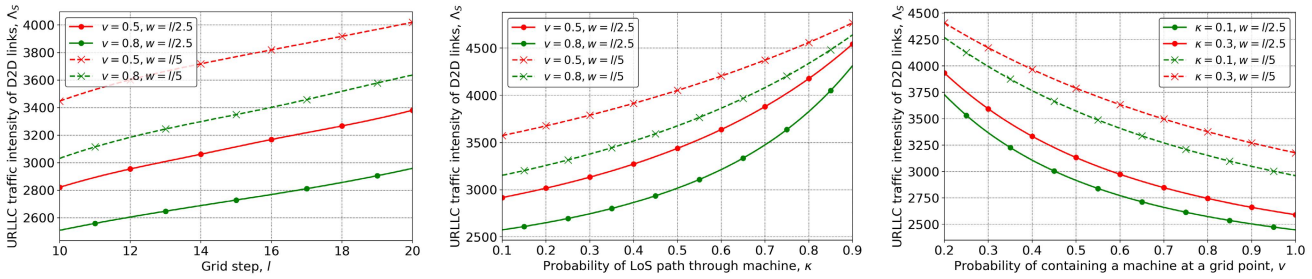

(a) As a function of l (b) As a function of κ (c) As a function of ν

FIGURE 9. Intensity of URLLC traffic that can be offloaded to D2D connections as a function of geometric deployment parameters.

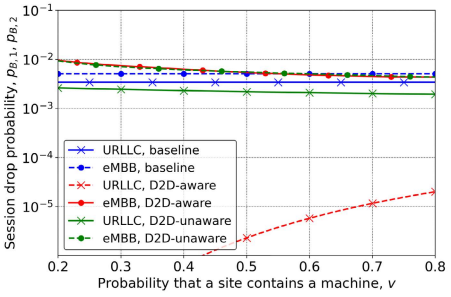

FIGURE 10. Session drop probability as a function of machine density.

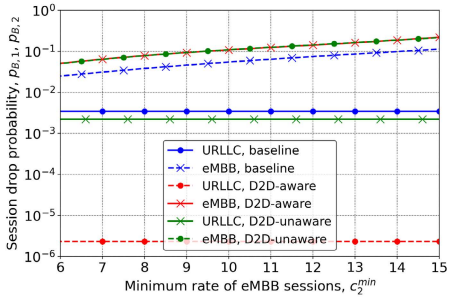

FIGURE 11. The effect of the minimum eMBB session rate.

B. PERFORMANCE OF CONSIDERED STRATEGIES

Having revealed the effect of environmental characteristics on D2D traffic intensity, we now evaluate the performance of considered service strategies. We start with Fig. 10 illustrating the session drop probability as a function of machine density regulated via probability that there is a machine at a site, ν for $c_1 = 2$ Mbps, $c_2^{\min} = 1$ Mbps, $N_A = 16$, $N_U = 4$, $\xi = 5 \times 10^{-4}$, $\mu_1 = 10^3$, $\mu_2 = 1/120$. Recall, that the increase of ν implies that the blockage probability increases, and thus the fraction of URLLC traffic that can be offloaded onto D2D connections decreases, see Fig. 9(c). Logically, the baseline scenario, where all the traffic goes through a BS, is characterized by constant eMBB and URLLC session drop probabilities. The former is an order of magnitude higher, which is explained by drastically different arrival rates and resource requirements. In its turn, the D2D-aware strategy, where a fraction of resources is allocated for direct connections and is not utilized at BS, is characterized by much smaller URLLC session drop probability reaching the required minimum of approximately 10^{-5} for $\nu = 0.5$. Then, it gradually increases but remains significantly smaller than that of the baseline strategy. Notably, the associated eMBB session drop probability remains comparable to that of the baseline strategy starting from $\nu = 0.5$. These gains come from D2D offloading.

Considering the last D2D-unaware strategy, one may observe that the gain of utilizing direct connections is negligible. Indeed, eMBB session drop probability is comparable to that of the baseline strategy, while the URLLC session drop probability decreases by no more than two times across the whole considered range of ν. The rationale is that in this strategy, the interference is uncontrolled and negatively impacts D2D connections in addition to URLLC session drop probability due to the lack of resources at BS. Under high load conditions considered here, this impact might be dramatic. In this context, it is logical to observe that the gap increases as ν becomes bigger. To validate these conclusions, we also illustrate the eMBB session preemption probability for all the considered strategies. Here, as one may observe, logically, eMBB session preemption probabilities coincide for D2D-aware and D2D-unaware strategies, implying that the fraction of URLLC traffic routed via BS experiences the same performance terms of dropped sessions and the performance degradation stems from interference. Thus, the major takeaway from the analysis performed above is that under high load conditions and dense scenarios making NR BS scheduling of D2D connection crucial even for directional mmWave systems.

EMBB sessions are inherently heavy-weight, producing a significant impact on the service performance of URLLC traffic. To this end, Fig. 11 shows the effect of the minimum requested rate of eMBB sessions on the session drop probabilities for $c_1 = 2$ Mbps, $N_A = 16$, $N_U = 4$, $\xi = 5 \times 10^{-4}$, $\mu_1 = 10^3$, $\mu_2 = 1/120$. As one may observe, the priority-based service manages to efficiently treat the case when the mean eMBB session requirements grow by keeping the URLLC session drop probability almost intact. Responding to the increased load is the eMBB session loss probability linearly increasing for all three considered strategies. Thus, the proposed priority-based method ensures that URLLC traffic is well-guarded from

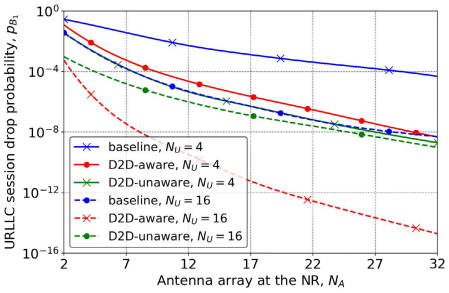

(a) URLLC drop probability

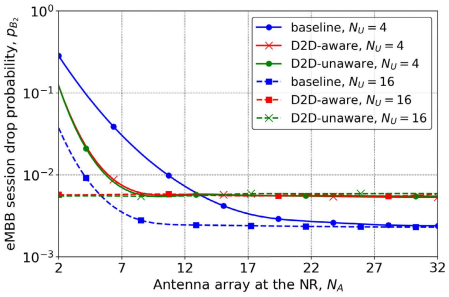

(b) eMBB drop probability

FIGURE 12. The effect of BS and UE arrays on session drop probabilities.

potentially fluctuating load of background traffic. Similar to the previous illustration, here, we also observe that D2D-aware strategy outperforms the rest of the considered strategies over the whole range of $c_2^{\min}$.

The use of directional antennas may produce a significant impact on the relative performance of the considered strategies. To assess their impact, Fig. 12 shows the impact of BS and UE antenna arrays on URLLC and eMBB session drop probabilities for $c_1 = 2$ Mbps, $c_2^{\min} = 1$ Mbps, $\xi = 5 \times 10^{-4}$, $\mu_1 = 10^3$, $\mu_2 = 1/120$. Analyzing the presented data, one may observe that the order of the curves in Fig. 12 is the same across all the considered values of the number of antenna elements implying that this parameter does not affect the choice of the best strategy identified in the previous discussion – D2D-aware strategy. However, the gain of utilizing the D2D-aware strategy drastically increases when the number of antenna elements at BS increases. For all the considered strategies, the number of antenna elements at both UE and BS sides affect the gains and thus the number of resources required to serve the traffic. As a result, both URLLC and eMBB session drop probabilities decrease as N_A or N_U increase. However, for the D2D-unaware strategy, the increased number of antenna elements also decreases the probability of interference, positively affecting the resulting URLLC session drop probability.

Analyzing Fig. 12 one may observe another interesting trend. Specifically, when the number of antenna elements utilized at BS antenna arrays reaches a certain value the eMBB session drop probability plateaus. The rationale is that when the number of antenna elements forming the antenna radiation pattern increases the quality of the received signal

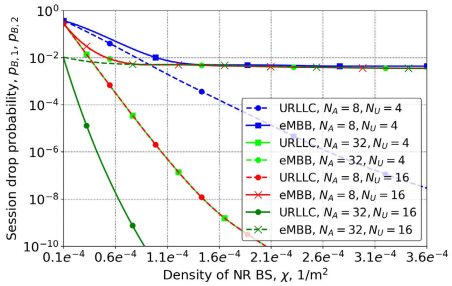

FIGURE 13. Drop probabilities as a function of deployment density.

increases as well (due to higher gain in transmit direction) decreasing the number of resources required for maintaining the minimum rate of eMBB sessions. This, when the number of antenna elements increases the eMBB drop probability plateaus. This number depends on other system parameters as well and can be computed by utilizing the proposed performance evaluation framework.

C. BS DEPLOYMENT DENSITY

Finally, we consider sample densities of BS deployments in industrial environments satisfying certain drop probabilities. These results are expected to be heavily influenced by all the considered system parameters, including environmental and system characteristics. To this end, Fig. 13 illustrates URLLC and eMBB session drop probabilities as a function of the BS density ξ and BS for all the considered strategies, selected BS antenna arrays, $c_1 = 2$ Mbps, $c_2^{\min} = 1$ Mbps, $\mu_1 = 10^3$, $\mu_2 = 1/120$. Expectedly, by increasing the density of BSs one minimizes URLLC session drop probability while eMBB session drop probability is only slightly affected.

VII. CONCLUSION

In this study, we have evaluated the coexistence between URLLC and eMBB traffic based on preemptive priority service discipline in realistic industrial deployments of mmWave 5G NR systems. To characterize the gains of the proposed solution, we have developed a detailed mathematical framework that captures both blockage and propagation conditions of mmWave band as well as the service prioritization between traffic types at NR BSs. We further evaluated three service strategies that utilize offloading of URLLC communications to the D2D links whenever possible. The main metric is the density of NR BSs required to serve the combination of URLLC and eMBB traffic with given performance guarantees. This metric is obtained numerically based on intermediate performance metrics that include session drop probabilities of both traffic types.

The presented numerical results show that the preemptive priority service discipline provides perfect isolation of high-priority latency-critical URLLC traffic from lower priority eMBB sessions. The D2D-aware strategy, where the BS explicitly reserves some resources for direct communications, drastically outperforms the one, where no explicit reservation is utilized as well as the baseline strategy, where all the traffic is routed through the NR BS. Furthermore, the

number of antennas heavily affects performance metrics in two ways – affecting the number of resources needed and impacting interference in D2D-unaware strategy. The proposed mathematical methodology can be utilized to estimate the required density of NR BS in industrial deployments such that performance guarantees for URLLC and eMBB traffic are satisfied.

ACKNOWLEDGMENT

This work was supported in part by the Russian Science Foundation (https://rscf.ru/en/project/21-19-00846/) under Grant 21-19-00846, in part by the Russian Science Foundation through the Sections I and II (https://rscf.ru/en/project/21-79-10139/) under Grant 21-79-10139, and in part by the RUDN University Strategic Academic Leadership Program (recipients Ekaterina Markova and Daria Ivanova, Section IV and V).

REFERENCES

[1] J. Navarro-Ortiz, P. Romero-Diaz, S. Sendra, P. Ameigeiras, J. J. Ramos-Munoz, and J. M. Lopez-Soler, "A survey on 5G usage scenarios and traffic models," *IEEE Commun. Surveys Tuts.*, vol. 22, no. 2, pp. 905–929, 2nd Quart., 2020.

[2] A. Ghosh, R. Ratasuk, and A. M. Rao, "Industrial IoT networks powered by 5G new radio," *Microw. J.*, vol. 62, no. 12, pp. 24–40, 2019.

[3] M. Gundall, J. Schneider, H. D. Schotten, M. Aleksy, D. Schulz, N. Franchi, N. Schwarzenberg, C. Markwart, R. Halfmann, P. Rost, and D. Wübben, "5G as enabler for industrie 4.0 use cases: Challenges and concepts," in *Proc. IEEE 23rd Int. Conf. Emerg. Technol. Factory Automat. (ETFA)*, vol. 1, Sep. 2018, pp. 1401–1408.

[4] S. Gangakhedkar, H. Cao, A. R. Ali, K. Ganesan, M. Gharba, and J. Eichinger, "Use cases, requirements and challenges of 5G communication for industrial automation," in *Proc. IEEE Int. Conf. Commun. Workshops (ICC Workshops)*, May 2018, pp. 1–6.

[5] F. Firyaguna, J. Kibilda, C. Galiotto, and N. Marchetti, "Performance analysis of indoor mmWave networks with ceiling-mounted access points," *IEEE Trans. Mobile Comput.*, vol. 20, no. 5, pp. 1940–1950, May 2021.

[6] V. Begishev, D. Moltchanov, E. Sopin, A. Samuylov, S. Andreev, Y. Koucheryavy, and K. Samouylov, "Quantifying the impact of guard capacity on session continuity in 3GPP new radio systems," *IEEE Trans. Veh. Tech.*, vol. 68, no. 12, pp. 12345–12359, Dec. 2019.

[7] K. Humadi, I. Trigui, W.-P. Zhu, and W. Ajib, "Dynamic base station clustering in user-centric mmWave networks: Performance analysis and optimization," *IEEE Trans. Commun.*, vol. 69, no. 7, pp. 4847–4861, Jul. 2021.

[8] N. H. Mahmood, M. Lopez, D. Laselva, K. Pedersen, and G. Berardinelli, "Reliability oriented dual connectivity for URLLC services in 5G new radio," in *Proc. 15th Int. Symp. Wireless Commun. Syst. (ISWCS)*, Aug. 2018, pp. 1–6.

[9] J. Rao and S. Vrzic, "Packet duplication for URLLC in 5G: Architectural enhancements and performance analysis," *IEEE Netw.*, vol. 32, no. 2, pp. 32–40, Mar./Apr. 2018.

[10] N. H. Mahmood, A. Karimi, G. Berardinelli, K. I. Pedersen, and D. Laselva, "On the resource utilization of multi-connectivity transmission for URLLC services in 5G new radio," in *Proc. IEEE Wireless Commun. Netw. Conf. Workshop (WCNCW)*, Apr. 2019, pp. 1–6.

[11] I. Gerasin, A. Krasilov, and E. Khorov, "Flexible multiplexing of grant-free URLLC and eMBB in uplink," in *Proc. IEEE 31st Annu. Int. Symp. Pers., Indoor Mobile Radio Commun.*, Aug. 2020, pp. 1–6.

[12] E. N. Tominaga, H. Alves, R. D. Souza, J. L. Rebelatto, and M. Latva-Aho, "Non-orthogonal multiple access and network slicing: Scalable coexistence of eMBB and URLLC," in *Proc. IEEE 93rd Veh. Technol. Conf. (VTC-Spring)*, Apr. 2021, pp. 1–6.

[13] P. Popovski, K. F. Trillingsgaard, O. Simeone, and G. Durisi, "5G wireless network slicing for eMBB, URLLC, and mMTC: A communication-theoretic view," *IEEE Access*, vol. 6, pp. 55765–55779, 2018.

[14] E. J. dos Santos, R. D. Souza, J. L. Rebelatto, and H. Alves, "Network slicing for URLLC and eMBB with max-matching diversity channel allocation," *IEEE Commun. Lett.*, vol. 24, no. 3, pp. 658–661, Mar. 2020.

[15] P. I. Tebe, K. Ntiamoah-Sarpong, W. Tian, J. Li, Y. Huang, and G. Wen, "Using 5G network slicing and non-orthogonal multiple access to transmit medical data in a mobile hospital system," *IEEE Access*, vol. 8, pp. 189163–189178, 2020.

[16] A. Banchs, G. de Veciana, V. Sciancalepore, and X. Costa-Perez, "Resource allocation for network slicing in mobile networks," *IEEE Access*, vol. 8, pp. 214696–214706, 2020.

[17] Y.-J. Chen, L.-Y. Cheng, and L.-C. Wang, "Prioritized resource reservation for reducing random access delay in 5G URLLC," in *Proc. IEEE 28th Annu. Int. Symp. Pers., Indoor, Mobile Radio Commun. (PIMRC)*, Oct. 2017, pp. 1–5.

[18] *NR; Physical Channels and Modulation (Release 15)*, document Rec. TR 38.211, 3GPP, Dec. 2017.

[19] N. Naddeh, S. B. Jemaa, S. E. Elayoubi, and T. Chahed, "Proactive RAN resource reservation for URLLC vehicular slice," in *Proc. IEEE 93rd Veh. Technol. Conf. (VTC-Spring)*, Apr. 2021, pp. 1–5.

[20] H. Ji, S. Park, J. Yeo, Y. Kim, J. Lee, and B. Shim, "Ultra-reliable and low-latency communications in 5G downlink: Physical layer aspects," *IEEE Wireless Commun.*, vol. 25, no. 3, pp. 124–130, Jun. 2018.

[21] *Release 15 Description; Summary of Rel-15 Work Items*, document 3GPP TR-21.915, 3GPP, Release 15, 2017.

[22] E. Markova, D. Moltchanov, R. Pirmagomedov, D. Ivanova, Y. Koucheryavy, and K. Samouylov, "Prioritized service of URLLC traffic in industrial deployments of 5G NR systems," in *Proc. Int. Conf. Distrib. Comput. Commun. Netw.* Cham, Switzerland: Springer, Sep. 2020, pp. 497–509.

[23] E. Markoval, D. Moltchanov, R. Pirmagomedov, D. Ivanova, Y. Koucheryavy, and K. Samouylov, "Priority-based coexistence of eMBB and URLLC traffic in industrial 5G NR deployments," in *Proc. 12th Int. Congr. Ultra Modern Telecommun. Control Syst. Workshops (ICUMT)*, Oct. 2020, pp. 1–6.

[24] W. Yang, C.-P. Li, A. Fakoorian, K. Hosseini, and W. Chen, "Dynamic URLLC and eMBB multiplexing design in 5G new radio," in *Proc. IEEE 17th Annu. Consum. Commun. Netw. Conf. (CCNC)*, Jan. 2020, pp. 1–5.

[25] S. R. Pandey, M. Alsenwi, Y. K. Tun, and C. S. Hong, "A downlink resource scheduling strategy for URLLC traffic," in *Proc. IEEE Int. Conf. Big Data Smart Comput. (BigComp)*, Feb. 2019, pp. 1–6.

[26] A. A. Esswie and K. I. Pedersen, "Opportunistic spatial preemptive scheduling for URLLC and eMBB coexistence in multi-user 5G networks," *IEEE Access*, vol. 6, pp. 38451–38463, 2018.

[27] A. A. Esswie and K. I. Pedersen, "Null space based preemptive scheduling for joint URLLC and eMBB traffic in 5G networks," in *Proc. IEEE Globecom Workshops (GC Wkshps)*, Dec. 2018, pp. 1–6.

[28] A. K. Bairagi, M. S. Munir, M. Alsenwi, N. H. Tran, S. S. Alshamrani, M. Masud, Z. Han, and C. S. Hong, "Coexistence mechanism between eMBB and uRLLC in 5G wireless networks," *IEEE Trans. Commun.*, vol. 69, no. 3, pp. 1736–1749, Mar. 2021.

[29] M. Alsenwi, N. H. Tran, M. Bennis, S. R. Pandey, A. K. Bairagi, and C. S. Hong, "Intelligent resource slicing for eMBB and URLLC coexistence in 5G and beyond: A deep reinforcement learning based approach," *IEEE Trans. Wireless Commun.*, vol. 20, no. 7, pp. 4585–4600, Jul. 2021.

[30] M. Alsenwi, N. H. Tran, M. Bennis, A. K. Bairagi, and C. S. Hong, "EMBB-URLLC resource slicing: A risk-sensitive approach," *IEEE Commun. Lett.*, vol. 23, no. 4, pp. 740–743, Apr. 2019.

[31] *Generic Network Slice Template*, document Rec. NG.116, V4.0, GSM Association, Nov. 2020. [Online]. Available: https://www.gsma.com/newsroom/wp-content/uploads//NG.116-v4.0-1.pdf

[32] Z. Kotulski, T. W. Nowak, M. Sepczuk, M. Tunia, R. Artych, K. Bocianiak, T. Osko, and J.-P. Wary, "Towards constructive approach to end-to-end slice isolation in 5G networks," *EURASIP J. Inf. Secur.*, vol. 2018, no. 1, pp. 1–23, Dec. 2018.

[33] R. Sabella, A. Thuelig, M. Carrozza, and M. Ippolito, "Industrial automation enabled by robotics, machine intelligence and 5G," *Ericsson Technol. Rev.*, vol. 2, pp. 1–13, 2018.

[34] J. Sachs, K. Wallstedt, F. Alriksson, and G. Eneroth, "Boosting smart manufacturing with 5G wireless connectivity," *Ericsson Tech. Rev.*, vol. 2, pp. 1–12, 2019.

[35] H. Kagermann, W. Wahlster, and J. Helbig, *Recommendations for Implementing the Strategic Initiative Industrie 4.0: Final Report of the Industrie 4.0 Working Group*. Munich, Germany: Acatech, 2013, pp. 19–26.

[36] *Service Requirements for Cyber-Physical Control Applications in Vertical Domains*, document Rec. TS 22.104 V17.2.0, 3GPP, Dec. 2019.

[37] J. Rambach, G. Lilligreen, A. Schäfer, R. Bankanal, A. Wiebel, and D. Stricker, "A survey on applications of augmented, mixed and virtual reality for nature and environment," in *Proc. Int. Conf. Hum.-Comput. Interact.* Cham, Switzerland: Springer, Jul. 2021, pp. 653–675.
[38] X. Zhang, Z. Cao, J. Li, D. Ge, Z. Chen, I. M. Vellekoop, and A. M. J. Koonen, "Wide-coverage beam-steered 40-Gbit/s non-line-of-sight optical wireless connectivity for industry 4.0," *J. Lightw. Technol.*, vol. 38, no. 24, pp. 6801–6806, Dec. 15, 2020.
[39] M. U. Sheikh, K. Ruttik, R. Jäntti, and J. Hämäläinen, "Blockage and ray tracing propagation model in 3GPP specified industrial environment," in *Proc. Int. Conf. Inf. Netw. (ICOIN)*, 2021, pp. 397–402.
[40] H. Tataria, K. Haneda, A. F. Molisch, M. Shafi, and F. Tufvesson, "Standardization of propagation models for terrestrial cellular systems: A historical perspective," *Int. J. Wireless Inf. Netw.*, vol. 28, no. 1, pp. 20–44, Mar. 2021.
[41] A. Orsino, R. Kovalchukov, A. Samuylov, D. Moltchanov, S. Andreev, Y. Koucheryavy, and M. Valkama, "Caching-aided collaborative D2D operation for predictive data dissemination in industrial IoT," *IEEE Wireless Commun.*, vol. 25, no. 3, pp. 50–57, Jun. 2018.
[42] R. Kovalchukov, D. Moltchanov, A. Samuylov, A. Ometov, S. Andreev, Y. Koucheryavy, and K. Samouylov, "Evaluating SIR in 3D millimeter-wave deployments: Direct modeling and feasible approximations," *IEEE Trans. Wireless Commun.*, vol. 18, no. 2, pp. 879–896, Feb. 2019.
[43] W. Feng, Y. Wang, D. Lin, N. Ge, J. Lu, and S. Li, "When mmWave communications meet network densification: A scalable interference coordination perspective," *IEEE J. Sel. Areas Commun.*, vol. 35, no. 7, pp. 1459–1471, Jul. 2017.
[44] *Study on Channel Model for Frequencies From 0.5 to 100 GHz (Release 14)*, document Rec. TR 38.901, V14.1.1, 3GPP, Jul. 2017.
[45] C. A. Balanis, "Antenna theory: Analysis and design," *Microstrip Antennas*, 3rd ed. Hoboken, NJ, USA: Wiley, 2005.
[46] A. M. Mathai, *An introduction to Geometrical Probability: Distributional Aspects With Applications*, vol. 1. Boca Raton, FL, USA: CRC Press, 1999.
[47] R. Schneider and W. Weil, *Stochastic and Integral Geometry*. Springer, Sep. 2008, p. 706.
[48] V. Petrov, D. Moltchanov, P. Kustarev, J. M. Jornet, and Y. Koucheryavy, "On the use of integral geometry for interference modeling and analysis in wireless networks," *IEEE Commun. Lett.*, vol. 20, no. 12, pp. 2530–2533, Dec. 2016.
[49] L. Lazos and R. Poovendran, "Stochastic coverage in heterogeneous sensor networks," *ACM Trans. Sensor Netw.*, vol. 2, no. 3, pp. 325–358, Aug. 2006.
[50] L. A. S. Sors and L. A. Santaló, *Integral Geometry and Geometric Probability*. Cambridge, U.K.: Cambridge Univ. Press, 2004.
[51] J. Wu, "On the primitive circle problem," *Monatshefte Math.*, vol. 135, no. 1, pp. 69–81, Feb. 2002.

DARIA IVANOVA received the M.Sc. degree in fundamental informatics from the Peoples' Friendship University of Russia (RUDN University), in 2020, where she is currently pursuing the Ph.D. degree with the Applied Probability and Informatics Department. Her research interests include wireless communications, mathematical modeling and performance analysis of 4G/5G networks, teletraffic theory, and queuing theory.

EKATERINA MARKOVA received the M.Sc. degree in applied mathematics and the Candidate of Science (Ph.D.) degree in applied mathematics and computer sciences from the Peoples' Friendship University of Russia (RUDN University), Russia, in 2011 and 2015, respectively. Since 2012, she has been working at the Telecommunication Systems Department, RUDN University. She is currently an Associate Professor with the Applied Probability and Informatics Department, RUDN University. She has coauthored multiple research works. Her current research interests include mathematical modeling and performance analysis of 5G networks, smart cities, spectrum sharing, multicast services, radio access, teletraffic theory, and queuing theory.

DMITRI MOLTCHANOV received the M.Sc. and Candidate of Science degrees from the St. Petersburg State University of Telecommunications, Russia, in 2000 and 2003, respectively, and the Ph.D. degree from the Tampere University of Technology, in 2006. He is currently a University Lecturer with the Laboratory of Electronics and Communications Engineering, Tampere University, Finland. He has (co)authored over 150 publications on wireless communications, heterogeneous networking, the IoT applications, and applied queuing theory. In his career he has taught more than 50 full courses on wireless and wired networking technologies, P2P/IoT systems, network modeling, and queuing theory. His current research interests include research and development of 5G/5G+ systems, ultra-reliable low-latency service, the industrial IoT applications, mission-critical V2V/V2X systems, and blockchain technologies.

RUSTAM PIRMAGOMEDOV received the M.Sc. and Candidate of Science degrees from the St. Petersburg State University of Telecommunications, Russia, in 2010 and 2014, respectively, and the D.Sc. degree from Tampere University, in 2020. From 2010 to 2018, he worked in engineering companies focused on the industrial IoT. Since 2018, he has been working as an Associate Rapporteur of Q9/11 at International Telecommunication Union. He is currently with Tampere University (TAU), Finland. His research interests include wireless communications, ICN, and the IoT.

YEVGENI KOUCHERYAVY received the Ph.D. degree from the Tampere University of Technology (TUT), Finland. He is currently a Professor at the Laboratory of Electronics and Communications Engineering, TUT. He is also with Kharkevich Institute for Information Transmission Problems, Russian Academy of Sciences. He is the author of numerous publications in the field of advanced wired and wireless networking and communications. His current research interests include various aspects in heterogeneous wireless communication networks and systems, the Internet of Things and its standardization, and nanocommunications. He is an Associate Technical Editor of the *IEEE Communications Magazine* and an Editor of the IEEE COMMUNICATIONS SURVEYS AND TUTORIALS.

KONSTANTIN SAMOUYLOV received the Ph.D. degree from Moscow State University and the Doctor of Sciences degree from the Moscow Technical University of Communications and Informatics. Since 2014, he has been the Head of the Department of Applied Informatics and Probability Theory, RUDN University (previously named PFUR). During last two decades, he has been conducting research projects for the Helsinki and Lappeenranta Universities of Technology, Moscow Central Science Research Telecommunication Institute, several Institutes of Russian Academy of Sciences, and a number of Russian network operators. He has written more than 150 scientific and technical articles and three books. His current research interests include performance analysis of 4G networks (LTE and WiMAX), teletraffic of triple play networks, signaling network (SIP) planning, and cloud computing.